OFDM vs. Single-Carrier Modulation: A New View on the PAR Behavior

Sebastian Stern and Robert F.H. Fischer
Institut für Nachrichtentechnik, Universität Ulm, Ulm, Germany
Email: {sebastian.stern, robert.fischer}@uni-ulm.de

***Abstract*— Since many years, the peak-to-average power ratio (PAR) behavior of single- and multi-carrier signals is controversially discussed in the literature. Thereby, the inferiority of multi-carrier transmission, in particular orthogonal frequency-division multiplexing (OFDM), was often stated. However, the generality of this assertion has to be doubted, as advanced single-carrier techniques have been ignored. In this paper, efficient approaches for the assessment of the PAR behavior for both modulation strategies are presented. In the single-carrier case, the impact of signal shaping on the constellation is assessed. On this basis, a meaningful comparison with OFDM based on identical spectral shapes is given, which enables a new point of view on the PAR performance of single- and multi-carrier schemes.**

I. Introduction

The assessment of the *peak-to-average power ratio* (PAR) of different modulation schemes has been of great interest over the last years, as the dimensioning of the power amplifier in the radio frontend eminently depends on the PAR behavior. More specifically, signal amplitudes exceeding the dimensioning of the amplifier may lead to signal distortions caused by non-linear effects (e.g., clipping [3]).

Consequently, a number of publications deal with the statistical distribution of the *instantaneous power* (IP), which is equivalent to the squared envelope of the transmit signal. For multi-carrier modulation, in particular *orthogonal frequency-division multiplexing* (OFDM), suitable approximations for the distribution of the IP can be found in the literature for quite a time, e.g., [6], [7], [16]. In the single-carrier case, approximations have been given first [14], [15], then exact approaches for the computation of distributions were presented [5], [8].

Regrettably, based on these references, there was no chance to compare the PAR behavior appropriately. The available approximations for OFDM consider the statistical properties of the discrete-time transmit signal or the continuous-time transmit signal obtained by ideal low-pass filtering. In contrast, for single-carrier modulation an ordinary transmit (pulse-shaping) filter is assumed, leading to different spectral shapes in both cases. Anyway, many authors claimed the superiority of single-carrier modulation with respect to the PAR behavior, e.g., in [14].

To overcome the shortcomings of the comparison, we recently proposed new efficient approaches to assess the IP distributions for (redundancy-free) single- and multi-carrier transmissions [13]. On this basis, single-carrier schemes like amplitude-shift keying (ASK) or quadrature-amplitude modulation (QAM) can adequately be compared to OFDM. These comparisons revealed that the PAR distributions are much more similar than often argued. Nevertheless, a remaining gap between single-carrier transmission and OFDM was figured out. This gap reflects the different distributions of the (time-domain) transmit symbols that are used as coefficients for pulse shaping, i.e., the transition from the discrete-time symbols to the continuous-time transmit signal. While, in the single-carrier case, these coefficients are directly drawn from a set of uniformly distributed signal points, by means of some "preprocessing" in OFDM (inverse discrete Fourier transform (IDFT)), a (nearly) continuous Gaussian distribution of these symbols is present there.

However, the assumption of uniformly distributed amplitude coefficients does not hold for all variants of single-carrier transmissions. For instance, the application of *signal shaping* [3]—a variant of preprocessing used to decrease the average transmit power—leads to (discrete) Gaussian distributed amplitude coefficients. Consequently, the statistical properties of constellation-shaped single-carrier signals will be quite similar to those of OFDM signals (discrete/continuous Gaussian distributed coefficients). However, still the question remains, whether shaping closes the gap between the PAR behavior of single- and multi-carrier schemes or affirms the inferiority of OFDM signals.

In this paper, we hence want to propose a method for the assessment of the PAR behavior if signal shaping is applied. This enables, in combination with procedures for the assessment of conventional single-carrier schemes and OFDM that are given in literature, a comparison between all above-mentioned variants of transmission. Furthermore, the impact of the signal shaping on both the average transmit power and the peak-to-average power will be discussed. Lastly, the question about an inferiority of single- or multi-carrier modulation will be clarified.

The paper is organized as follows: In Section II, the system model is given for all above-mentioned modulation techniques. Section III starts with elementary statistical properties and definitions, following scheme-specific strategies for an efficient and precisely assessment of the related distributions of instantaneous power. Based on these considerations, numerical results are presented in Section IV. Moreover, the different modulation methods are compared in regard to their PAR behavior and several influencing factors. Finally, the paper closes with a brief conclusion (Section V).

II. System Model

All transmission schemes that are discussed in this paper can be seen as variants of *pulse-amplitude modulation* (PAM). The block diagram of a PAM transmitter is depicted in Fig. 1.

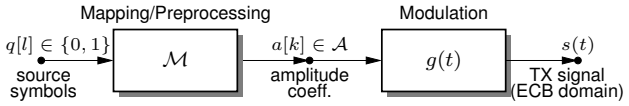

Fig. 1. Transmitter model for PAM transmission.

A redundancy-free sequence of source symbols $q[l] \in \{0,1\}$, $l \in \mathbb{Z}$ (bits) has to be communicated. Depending on the specific modulation scheme, these source symbols are mapped to discrete-time amplitude coefficients $a[k]$, $k \in \mathbb{Z}$ (possibly by some means of preprocessing or an advanced mapping procedure). Following this, these coefficients serve as basis for obtaining the continuous-time transmit signal in the equivalent complex baseband (ECB) [3]. The ECB signal is formed by pulse-shaping according to

$$s(t) = \sum_{k=-\infty}^{\infty} a[k]\, g(t - kT)\ , \tag{1}$$

where T denotes the symbol interval and $g(t)$ the impulse response of the pulse-shaping filter. The pulse-shaping can be regarded as a filtering of the discrete-time sequence of amplitude coefficients with a continuous-time pulse $g(t)$.

A square-root-raised-cosine (RRC) pulse shape with some roll-off factor $\alpha \in [0,1]$ is assumed throughout the paper; its energy is denoted as E_g. Its impulse response with normalization constant $c = \sqrt{E_\mathrm{g}/T}$ is given by [10]

$$g(t) = c \cdot \frac{4\alpha t \cos(\pi(1+\alpha)t/T) + T\sin(\pi(1-\alpha)t/T)}{\pi t(1-(4\alpha t/T)^2)}\ . \tag{2}$$

Noteworthy, the choice of a square-root-raised-cosine pulse ensures the fulfillment of the *Nyquist condition for zero intersymbol interference* [10] if a matched-filter is applied at the receiver.

Since (2) gives an impulse response of infinite duration, for practical considerations, $g(t)$ has to be limited to a finite length. To this end, we assume

$$\forall t \notin \left[-\frac{K}{2}T, \frac{K}{2}T\right) :\ g(t) = 0\ , \tag{3}$$

with $K \in \mathbb{N}$ and K even. As the associated loss of energy is negligible for sufficiently large values of K, referring to [13], $K = 2000$ is chosen for the numerical evaluations of this paper.

The procedure of pulse shaping described by (1) basically does not differ between conventional single-carrier modulation schemes like ASK or QAM, advanced single-carrier processing using signal shaping, and multi-carrier transmission via OFDM. However, the statistical properties[1] of the amplitude coefficients $a[k]$ largely depend on the kind of mapping/preprocessing strategy which is applied to obtain the coefficients out of the source symbols. In the following, the different strategies are explained in detail, especially with regard to the particular impact on the amplitude coefficients' statistics.

[1]The sequence $q[l]$ is a discrete-time stationary random process, thus, $a[k]$ is also a discrete-time stationary random process, and $s(t)$ a continuous-time cyclostationary random process.

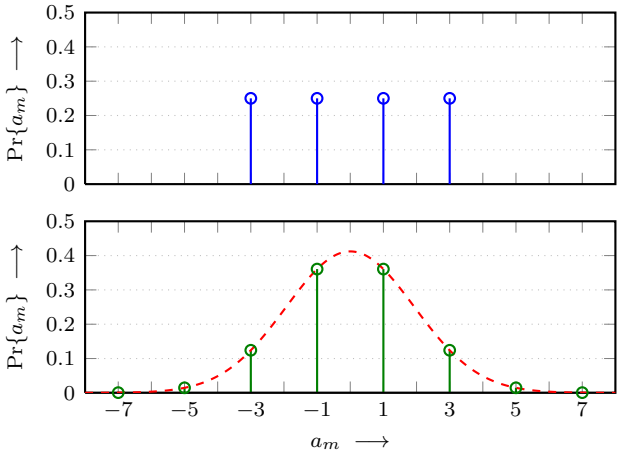

Fig. 2. Distribution of coefficients $a[k]$ for rate $R = 2$. Top: Discrete uniform distribution (4ASK). Bottom: Discrete Gaussian distribution obtained by signal shaping based on eight coefficients.

A. Conventional Single-Carrier Modulation

In case of conventional single-carrier methods, the source symbols are directly mapped to symbols, drawn from a set $\mathcal{A} = \{a_m\}$ of real- (ASK) or complex-valued (QAM) amplitude coefficients with cardinality $M = |\mathcal{A}|$ (cf. Fig. 1). We restrict ourselves to zero-mean constellations. The rate of the modulation scheme is then given as $R = \log_2(M)$ bits per symbol. For bipolar ASK, the set of coefficients (constellation) reads

$$\mathcal{A}_\mathrm{ASK} \stackrel{\text{def}}{=} \Big\{ \underbrace{(2m - (M+1))}_{a_m} \ \Big|\ m \in \{1,\ldots,M\} \Big\}\ , \tag{4}$$

whereas for square QAM ($\sqrt{M} \in \mathbb{N}$), the complex-valued coefficients are formed via

$$a[k] = a_\mathrm{I}[k] + \mathrm{j}\, a_\mathrm{Q}[k]\ , \tag{5}$$

assuming that $\mathcal{A}_\mathrm{I} = \mathcal{A}_\mathrm{Q} = \{a_1,\ldots,a_{\sqrt{M}}\}$.

Due to the redundany-free sequence of bits $q[l]$, all amplitude coefficients $a[k]$ are independent and identically distributed (i.i.d.). In particular, they possess a discrete uniform distribution as shown in Fig. 2 (top) for 4ASK. The variance of the constellation[2]

$$\sigma_a^2 \stackrel{\text{def}}{=} \mathrm{E}\{|a[k]|^2\}\ , \tag{6}$$

which is equivalent to the average symbol energy, is given as $\sigma_a^2 = (M^2-1)/3$ in case of ASK and $\sigma_a^2 = 2(M-1)/3$ for QAM.

[2]Notation: $\Pr\{\cdot\}$ denotes probability, $\mathrm{E}\{\cdot\}$ expectation.

B. Signal Shaping for Single-Carrier Modulation

In contrast to classical single-carrier modulation, signal shaping can be considered as an advanced mapping procedure. A desired transmission rate R (bits per symbol/amplitude coefficient) has to be communicated. To this end, a set of coefficients $\tilde{\mathcal{A}}$ is chosen according to (4) or (5), respectively, though, with extended cardinality $|\tilde{\mathcal{A}}| \stackrel{\text{def}}{=} \tilde{M} \geq 2^R$. Instead of drawing these coefficients uniformly, their probabilities are selected in such a way that the constellation's entropy $H(\tilde{\mathcal{A}})$ equals the desired rate R, mathematically

$$H(\tilde{\mathcal{A}}) = \sum\nolimits_{a_m \in \tilde{\mathcal{A}}} \Pr\{a_m\} \log_2(\Pr\{a_m\}) \stackrel{!}{=} R \,. \quad (7)$$

The purpose of the above-mentioned approach is the decrease of the average symbol energy compared to ASK/QAM constellations of the same rate, which can be expressed by the shaping gain

$$G_\mathrm{s} \stackrel{\text{def}}{=} \frac{\sigma_a^2}{\tilde{\sigma}_a^2} \,, \quad (8)$$

where σ_a^2 denotes the average energy of the original constellation and $\tilde{\sigma}_a^2$ the average energy of the shaped one. It can be proven that a (discrete) Gaussian distribution maximizes the achievable shaping gain [3].

Fig. 2 (bottom) depicts the optimal distribution for the parameters $R = 2$ and $\tilde{M} = 8$. Obviously, this probability mass function approximates a (suitably chosen) Gaussian probability density function (red curve). For the considerations in this paper, we restrict to optimal shaped constellations and i.i.d. coefficients; specific shaping/mapping algorithms are not of interest.

C. Orthogonal Frequency-Division Multiplexing

Even though there is a conceptual difference between single- and multi-carrier modulation schemes, OFDM can be considered as a special kind of PAM transmission applying some means of multi-carrier preprocessing. Fig. 3 shows the block diagram of an OFDM transmitter.

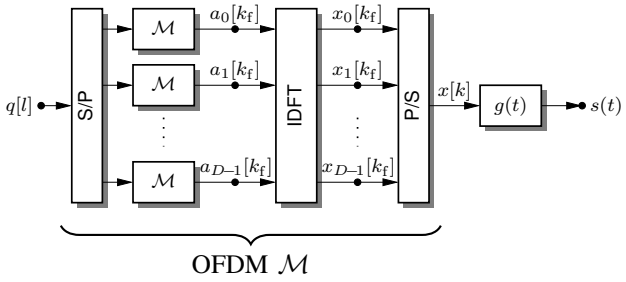

Fig. 3. Transmitter model for OFDM transmission.

Initially, the (redundancy-free) sequence of bits is split into D parallel streams ($\widehat{=}$ subcarriers) by serial-to-parallel (S/P) conversion. These bit streams are subsequently mapped to signal points of a given constellation $\mathcal{A}$ analogous to conventional single-carrier mapping (e.g., QAM). W.l.o.g., we assume the same constellation/mapping for every parallel stream. As an outcome, a vector $\boldsymbol{a}[k_\mathrm{f}] = [a_0[k_\mathrm{f}], \ldots, a_{D-1}[k_\mathrm{f}]]$ of frequency-domain data symbols is formed (called *frame*), k_f denoting the actual frame number. Afterwards, the IDFT

$$x_l[k_\mathrm{f}] = \frac{1}{D} \sum_{j=0}^{D-1} a_j[k_\mathrm{f}] \cdot \mathrm{e}^{\mathrm{j}\frac{2\pi}{D} jl}, \quad l \in \{0, \ldots, D-1\} \quad (9)$$

is employed in order to compute a corresponding frame of time-domain symbols $\boldsymbol{x}[k_\mathrm{f}] = [x_0[k_\mathrm{f}], \ldots, x_{D-1}[k_\mathrm{f}]]$. Using a parallel-to-serial (P/S) converter, these frames are parallel/serial converted to a sequence $x[k]$ of time-domain symbols which serve as amplitude coefficients for the pulse shaping according to (1), obtaining the transmit signal $s(t)$ in ECB domain. Hence, the symbols accomplish exactly the same purpose as the directly (or via signal shaping) drawn coefficients $a[k]$ in the single-carrier case. The entirety of processing steps can thus be seen as a specific OFDM mapping[3] (cf. Fig. 3) to gain amplitude coefficients for pulse-shaping out of source symbols.

Nevertheless, the multi-carrier preprocessing results in particular circumstances for statistical analysis. Assuming a large amount of parallel streams (subcarriers, e.g., $D \geq 128$), as relevant for practical purposes, the addition of i.i.d. frequency-domain symbols in (9) approximately leads to a complex continuous Gaussian distribution of the time-domain symbols $x[k]$ according to the central limit theorem [9], [12]. The time-domain symbols are well approximated to be mutually independent, each with independent real and imaginary parts [11], [13]. Consequently, for statistical considerations, OFDM is equivalent to single-carrier transmissions with complex Gaussian amplitude coefficients [12], [13].

It should also be noted that usually not all of the frequency-domain symbols of the frames $\boldsymbol{a}[k_\mathrm{f}]$ are used for data transmission, but some of them are set to zero in order to form the OFDM *guard bands* [1]. This practice leads to benefits concerning the power spectral density (PSD) of the transmit signal, which is depicted in Fig. 4. In case of single-carrier PAM or OFDM without guard bands (Fig. 4 top), a constant PSD $\Phi_{aa}(\mathrm{e}^{\mathrm{j}2\pi fT})$ of the discrete time stationary process $a[k]$ (respectively $x[k]$ for OFDM) is given due to i.i.d. zero-mean coefficients. As a consequence, the (time-averaged) PSD $\bar{\Phi}_{ss}(f)$ of the continuous-time process $s(t)$ is proportional to the energy spectral density $|G(f)|^2$ of the basic pulse shape $g(t)$. By contrast, the application of OFDM guard bands (Fig. 4 bottom) results in frequency band where the PSD of the discrete-time sequence of time-domain symbols is (nearly) zero. If the non-modulated subcarriers and the pulse shape are suitably chosen, there is the chance to achieve an almost rectangular PSD $\bar{\Phi}_{ss}(f)$ without significant effort for filtering. For single-carrier modulation, an equivalent spectral shape could only be achieved by virtually ideal

[3] As usual in the related literature about PAR behavior, the OFDM guard interval [1] is neglected.

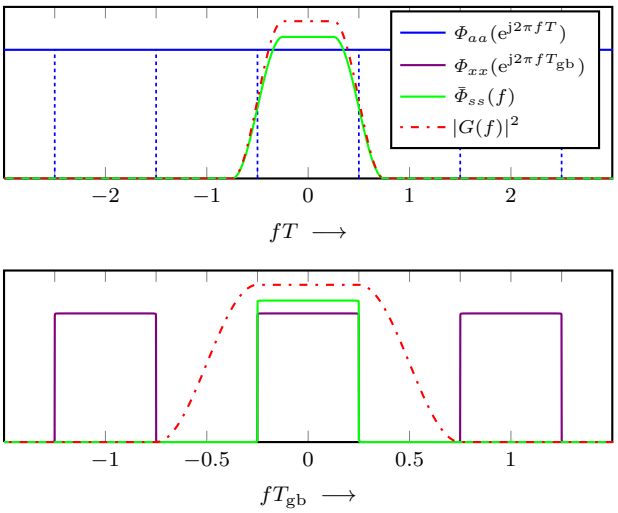

Fig. 4. Time-averaged power spectral densities $\bar{\Phi}_{ss}(f)$ in dependency of $\Phi_{aa}(\mathrm{e}^{\mathrm{j}2\pi fT})$ or $\Phi_{xx}(\mathrm{e}^{\mathrm{j}2\pi fT_{\mathrm{gb}}})$ and $|G(f)|^2$ (RRC pulse shape, $\alpha = 0.5$). Top: PSD of single-carrier PAM modulation and OFDM ($a[k] \mathrel{\widehat{=}} x[k]$) without guard bands. Bottom: PSD of OFDM transmission with guard bands (half of the subcarriers set to zero, hence $T_{\mathrm{gb}} = T/2$).

low-pass filtering (RRC with $\alpha \approx 0$). Certainly, the above-mentioned strategy is accompanied by a decrease in data rate, which can be compensated by a shortening of the the symbol interval T to a new interval T_{gb}. Further details about this approach in general, which can be considered as an oversampling, and its consequences regarding the PAR behavior are mentioned in [13].

III. Theoretical Considerations for the Assessment of PAR Behavior

In this section, strategies for an accurate and efficient assessment of the PAR behavior and the computation of the IP distributions are presented. For that purpose, we concentrate on the theoretical backgrounds in order to derive the statistical distributions of each modulation scheme which is discussed in the paper.

As already mentioned before, we are interested in statistical characteristics of the instantaneous power $p(t) \mathrel{\overset{\text{def}}{=}} |s(t)|^2$. More precisely, the *normalized instantaneous power*

$$p_{\mathrm{n}}(t) \mathrel{\overset{\text{def}}{=}} \frac{p(t)}{\mathrm{E}\{p(t)\}} = \frac{p(t)}{\sigma_a^2 E_{\mathrm{g}}/T} \tag{10}$$

is suited to achieve a comparability between different modulation methods and transmission parameters owing to a normalization to the average transmit power. Generally, $s(t)$ and by association $p_{\mathrm{n}}(t)$ are *cyclostationary random processes* [4], [13], i.e., the processes are non-stationary but their statistical properties periodically repeat with period T. Therefore, the analysis can be confined to $t \in [0, T)$.

It is common practice to assess the PAR behavior via the *complementary cumulative distribution function* (ccdf), which is defined as

$$\Gamma_{p_{\mathrm{n}}}(\hat{p}_{\mathrm{n}}, t) \mathrel{\overset{\text{def}}{=}} \Pr\{p_{\mathrm{n}}(t) \geq \hat{p}_{\mathrm{n}}\} \,, \tag{11}$$

$\hat{p}_{\mathrm{n}}$ denoting a certain value/threshold. In this manner, we can evaluate the probability of occurrence concerning large values of (normalized) IP. The cyclostationarity of the random process is taken into account by considering the time-averaged ccdf

$$\Gamma_{\bar{p}_{\mathrm{n}}}(\hat{p}_{\mathrm{n}}) \mathrel{\overset{\text{def}}{=}} \frac{1}{T} \int_0^T \Gamma_{p_{\mathrm{n}}}(\hat{p}_{\mathrm{n}}, t) \, \mathrm{d}t \,. \tag{12}$$

Furthermore, referring to [13], the *inverse ccdf* (iccdf)

$$\Gamma^{-1}_{\bar{p}_{\mathrm{n}}}(\psi) \mathrel{\overset{\text{def}}{=}} \inf\{\hat{p}_{\mathrm{n}} \in \mathbb{R}_0^+ \mid \Gamma_{\bar{p}_{\mathrm{n}}}(\hat{p}_{\mathrm{n}}) \leq \psi\} \tag{13}$$

yields the value of IP which is exceeded with a given probability $\psi \in [0, 1]$, e.g., $\psi = 10^{-6}$. Assessing the PAR behavior of modulation schemes via iccdf is much more convenient than the comparison of maximum peak values, as the maximum values possess no practical relevance due to their extremely low probabilities.

On the basis of the restriction to $t \in [0, T)$ and a basic pulse shape with finite duration KT (cf. (3)), there is the chance to simplify the pulse shaping given in (1) for further calculations [8], [13], [14]. Hence, we substitute all involved amplitude coefficients by $a_\kappa \mathrel{\overset{\text{def}}{=}} a[\kappa - K/2]$ and the filter coefficients by $g_\kappa(t) \mathrel{\overset{\text{def}}{=}} g(t - (\kappa - K/2)T)$, with index $\kappa \in \{1, \ldots, K\}$. In this means, (1) can be rewritten as

$$s(t) = \sum_{\kappa=1}^{K} a_\kappa \, g_\kappa(t) \,, \quad t \in [0, T) \,. \tag{14}$$

Moreover, the products of amplitude coefficients a_κ and time-dependent filter coefficients $g_\kappa(t)$ are shortened by

$$s_\kappa(t) \mathrel{\overset{\text{def}}{=}} a_\kappa \, g_\kappa(t) \,. \tag{15}$$

A. Conventional Single-Carrier Modulation

For the assessment of the PAR behavior with regard to ASK and QAM, we relate to the approach presented in [13]. Thus, the evaluation of characteristic functions [9] allows an exact computation of the related distributions of instantaneous power.

More specifically, we are interested in the characteristic functions (the inverse Fourier transform of the pdf) of the products $s_\kappa(t)$, defined by

$$\varphi_{s_\kappa}(\omega, t) \mathrel{\overset{\text{def}}{=}} \mathrm{E}\{\mathrm{e}^{\mathrm{j}\omega s_\kappa(t)}\} = \int_{-\infty}^{\infty} f_{s_\kappa}(\hat{s}, t) \cdot \mathrm{e}^{\mathrm{j}\omega\hat{s}} \, \mathrm{d}\hat{s} \,, \tag{16}$$

where $f_{s_\kappa}(\hat{s}, t)$ denotes the probability density function (pdf) of $s_\kappa(t)$.

Considering M-ary ASK with uniformly drawn coefficients, the characteristic function can easily be deduced as

$$\varphi_{s_\kappa}(\omega, t) = \frac{2}{M} \sum_{m=1}^{M/2} \cos(\omega a_m g_\kappa(t)) \,. \tag{17}$$

For the hypothetical case of $M \to \infty$, the pdf approaches a uniform distribution within the interval $[-\sqrt{3}, \sqrt{3}]$ (such

that $\sigma_a^2 = 1$) [13], [14]. The characteristic function then reads[4]

$$\varphi_{s_\kappa}(\omega, t) = \mathrm{si}(\omega\sqrt{3}g_\kappa(t)) \; . \tag{18}$$

Taking advantage of the property that the addition of independent random variables (cf. (14)) leads to the multiplication of their characteristic functions, the (ECB) transmit signal possesses the characteristic function

$$\varphi_s(\omega, t) = \prod_{\kappa=1}^{K} \varphi_{s_\kappa}(\omega, t) \; . \tag{19}$$

With the aid of the Fourier transform, a corresponding pdf $f_s(\hat{s}, t)$ can be calculated, providing the basis for obtaining the ccdf

$$\Gamma_s(\hat{s}, t) = \int_s^\infty f_s(\xi, t) \, \mathrm{d}\xi \; . \tag{20}$$

The related ccdf of the normalized instantaneous power is subsequently formed by [13]

$$\Gamma_{p_\mathrm{n}}(\hat{p}_\mathrm{n}, t) = 2\,\Gamma_s\left(\sqrt{\hat{p}_\mathrm{n}\sigma_a^2 E_\mathrm{g}/T}, t\right) \; . \tag{21}$$

Finally, the cyclostationarity of the transmit signal is taken into account by time-averaging according to (12), yielding the ccdf $\Gamma_{\bar{p}_\mathrm{n}}(\hat{p}_\mathrm{n})$.

The above-mentioned strategy holds the benefit of an extensibility to square QAM constellations. To this end, the given procedure is performed for both the real and imaginary part of $s(t)$, resulting in characteristic functions for both components (that are exactly the same). Since $p(t) = |s(t)|^2 = s_\mathrm{I}^2(t) + s_\mathrm{Q}^2(t)$, the pdf of the instantaneous power can be acquired by the convolution of the associated pdfs, which corresponds to an additional multiplication of characteristic functions. More details about this strategy are mentioned in [13].

B. Signal Shaping for Single-Carrier Modulation

The approach based on characteristic functions is also suited for the assessment of the PAR behavior if signal shaping is applied, as the basic practice does not differ from conventional schemes like ASK or QAM. To be exact, the characteristic functions of the products $s_\kappa(t)$ are the only quantities that have to be adjusted to the properties that occur due to shaping.

For one-dimensional shaped constellations, the characteristic function is then determined as

$$\varphi_{s_\kappa}(\omega, t) = 2 \sum_{m=1}^{\tilde{M}/2} \Pr\{a_m\} \cdot \cos(\omega a_m g_\kappa(t)) \; . \tag{22}$$

As easy to recognize, (22) is a generalized form of (17), adapted to amplitude coefficients with different probabilities of occurrence. In the two-dimensional case, (22) is again evaluated for both dimensions separately, following a multiplication of the two characteristic functions.

[4]The sinc function is defined as $\mathrm{si}(x) \stackrel{\mathrm{def}}{=} \frac{\sin(x)}{x}$.

In theory, continuous Gaussian distributed coefficients would be the constellation obtaining the maximum achievable shaping gain [3]. In that case, an analytical expression for the ccdf of the normalized instantaneous power can be established. For that purpose, we assume zero-mean real Gaussian coefficients, each with variance σ_a^2. As pulse shaping can simply be seen as a filter operation, the Gaussian shape is maintained, and the variance is given by

$$\sigma_s^2(t) \stackrel{\mathrm{def}}{=} \mathrm{E}\{|s(t)|^2\} = \sigma_a^2 \sum_{\kappa=1}^{K} g_\kappa^2(t) \; . \tag{23}$$

Hence, since a Gaussian distribution is completely described by the variance (and the mean-value), the distribution of a certain instance of time just depends on the related filter coefficients, and the ccdf of the normalized IP reads[5]

$$\Gamma_{p_\mathrm{n}}(\hat{p}_\mathrm{n}, t) = \mathrm{erfc}\left(\frac{\sqrt{\hat{p}_\mathrm{n} E_\mathrm{g}/T}}{\sqrt{2\sum_{\kappa=1}^{K} g_\kappa^2(t)}}\right) \; . \tag{24}$$

If we consider, by contrast, complex Gaussian coefficients (with independent components and all-over variance σ_a^2), the circumstances change as follows: Here, $|s(t)|$ possesses a Rayleigh distribution [9], [13] with the time-dependent scale-parameter $\sigma_\mathrm{r}^2 = \sigma_a^2/2 \cdot \sum_{\kappa=1}^{K} g_\kappa^2$. As a consequence, we obtain an exponential distribution for the normalized IP with ccdf

$$\Gamma_{p_\mathrm{n}}(\hat{p}_\mathrm{n}, t) = \exp\left(-\frac{\hat{p}_\mathrm{n} E_\mathrm{g}/T}{\sum_{\kappa=1}^{K} g_\kappa^2}\right) \; . \tag{25}$$

Therefore, in case of real- or complex-valued Gaussian coefficients, the numerical evaluation of (24) or (25) in combination with time-averaging is sufficient for the calculation of the desired normalized ccdf $\Gamma_{\bar{p}_\mathrm{n}}(\hat{p}_\mathrm{n})$.

C. Orthogonal Frequency-Division Multiplexing

In OFDM transmission, rotationally-invariant complex Gaussian time-domain symbols/coefficients are (approximately) generated, cf. Section II. Hence, the same situation as for ideal signal shaping is present; $|s(t)|$ is well approximated by a Rayleigh distribution and the normalized instantaneous power is exponentially distributed, cf. (25).

However, there is a significant difference between (theoretical) OFDM modulation assuming all of the available subcarriers to be employed for data transmission, and OFDM involving the application of guard bands. In the first-mentioned case, the non-rectangular power spectral density (assuming $\alpha \gg 0$) is accompanied by a cyclostationary transmit signal $s(t)$, like in the single-carrier case. In contrast, the guard bands allow the generation of a rectangular spectral shape, leading to a wide-sense stationary signal, which means that the variance of the Gaussian distribution (hence, average transmit power) is

[5]$\mathrm{erfc}(x) = \frac{2}{\sqrt{\pi}} \int_x^\infty \mathrm{e}^{-\xi^2} \, \mathrm{d}\xi$ is the complementary error function.

constant over time, and hence is the distribution. The impact of the stationarity on the PAR behavior will be discussed in the following section. Under the above-mentioned conditions, the time-averaged ccdf of OFDM modulation is well approximated by [13]

$$\Gamma_{\bar{p}_\mathrm{n}}(\hat{p}_\mathrm{n}) = \mathrm{e}^{-\hat{p}_\mathrm{n}} \ . \tag{26}$$

IV. Numerical Results and Comparison

The strategies and procedures introduced in the last section are now used for numerical evaluations. To this end, the ccdf and the iccdf are employed as means for comparisons between different modulation schemes and they serve for the discussion on influencing factors. Moreover, since the impact of signal shaping on the PAR behavior has not been discussed in the literature yet, Monte-Carlo simulations are conducted to support the theoretical considerations.

For the computation of the cddfs and iccdfs that are given in the following, the numerical approach in [13] was used in case of single-carrier modulation (with and without signal shaping). Thus, the fast Fourier transform (FFT) was selected as numerical implementation[6] of the Fourier transform (cf. (16)). Furthermore, the time-averaging, i.e., the integral in (12), is numerically approximated by 128 equidistant sampling points within $t \in [0, T)$. In contrast, for Gaussian coefficients, the distributions are directly computed through the evaluation of the related analytical expressions.

Fig. 5 depicts the ccdf of the normalized IP for rate $R = 2$ (4ASK as baseline), RRC pulse shape with $\alpha = 0.45$ and real-valued transmission. For comparison, the ccdf of ASK modulation in case of $M \to \infty$ is also shown, since it is associated with worst-case PAR statistics for conventional real-valued modulation. In addition, the ccdfs for shaped constellations, namely $\tilde{M} = 8$ and $\tilde{M} = 12$ discrete Gaussian coefficients, are illustrated. For $\tilde{M} = 8$, the numerically computed curve perfectly matches that determined by Monte-Carlo simulation. Noteworthy, the shaped constellations exhibit nearly the same distribution as continuous (real-valued) Gaussian coefficients, marginal deviations arise as a result of the shaped constellations' discrete character. Besides, the gap of about 1.5 dB concerning shaping with $\tilde{M} = 8$ and $\tilde{M} = 12$ for low probabilities (about 10^{-6}), can be explained regarding the four additional high-amplitude coefficients. An enormous difference of about 7 to 8 dB compared to 4ASK and of about 6 to 7 dB to a uniform continuous constellation can be observed.

The impact of signal shaping is further analyzed in Fig. 6, where the iccdf for a probability $\psi = 10^{-6}$ is shown in dependency of the roll-off factor α for the above-mentioned real-valued modulation formats of rate $R = 2$. First, we are able to recognize the typical property of conventional single-carrier modulation: The best achievable PAR behavior is given for $\alpha \approx 0.45$, which can be explained by the influence of the roll-off factor on the cyclostationarity of the transmit signal [13].

[6]The number of samples and the representing values were chosen such that numerical effects accompanied by the FFT (cyclic convolution, leakage) were avoided or minimized.

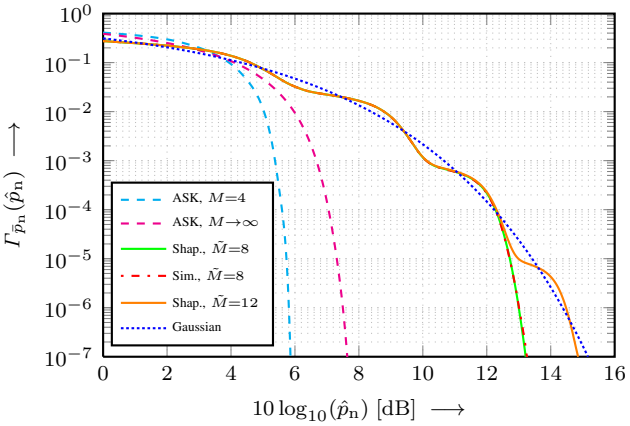

Fig. 5. Time-averaged ccdf of the normalized instantaneous power for real-valued modulation of rate $R = 2$ (RRC, $\alpha = 0.45$). In case of shaping with $\tilde{M} = 8$, the results from Monte-Carlo simulation are also shown.

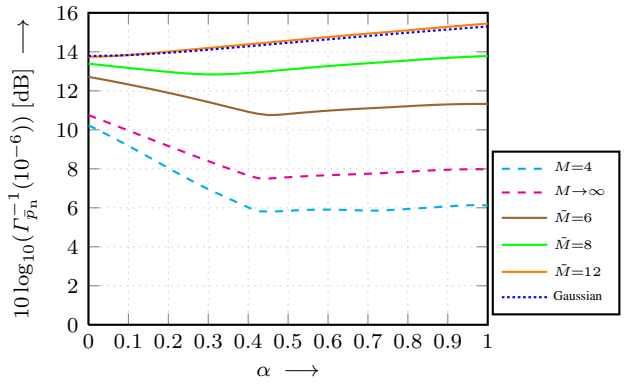

Fig. 6. Time-averaged iccdf of the normalized instantaneous power at probability $\psi = 10^{-6}$ over the roll-off factor α. Real-valued modulation with rate $R = 2$. Dashed (cyan, magenta): conventional ASK; solid: shaped constellations; dotted blue: one-dimensional continuous Gaussian pdf.

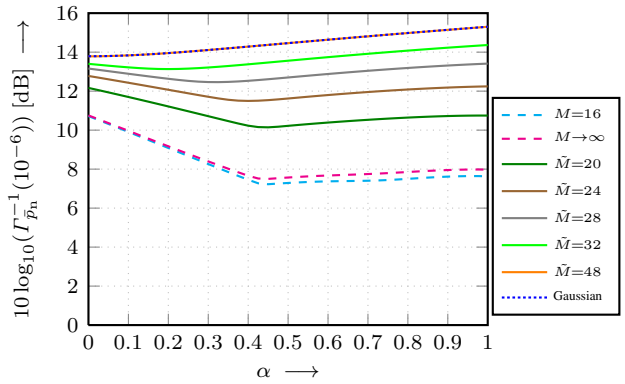

Fig. 7. Time-averaged iccdf of the normalized instantaneous power at probability $\psi = 10^{-6}$ over the roll-off factor α. Real-valued modulation with rate $R = 4$. Dashed (cyan, magenta): conventional ASK; solid: shaped constellations; dotted blue: one-dimensional continuous Gaussian pdf.

Contrary to this, for the continuous Gaussian distribution the lowest PAR values are obtained in case of ideal low-pass filtering. Here, a wide-sense stationary transmit signal and, hence, a time-independent distribution (cf. Section III) result, which is the best case for Gaussian coefficients [13]. Considering the curves of the iccdf for the shaped constellations, we see again the degrading PAR behavior when increasing the constellation expansion; in the limit a nearly continuous Gaussian statistic is reached. In turn, best PAR performance is obtained for decreasing α when increasing the size of the constellation.

Fig. 8 depicts the ccdf curves for the complex-valued case; the same constellations as in Fig. 5 are used per quadrature component, leading to the rate $R = 4$ (16QAM as baseline). Again, the numerically computed ccdf and the one obtained by Monte-Carlo simulation match very well. All observations and conclusions are basically identical compared to real-valued coefficients. However, complex-valued constellations show a superior PAR behavior in general and the shaped constellations approach the (two-dimensional) continuous Gaussian distribution faster. This can also be seen in Fig. 9, where the associated iccdf curves are given. The shaped constellation with $\tilde{M} = 36$ coefficients (i.e., $1.5\times$ the cardinality per dimension compared to 16QAM) possesses a nearly constant iccdf over α. For $\tilde{M} = 144$ (i.e., $3\times$ the cardinality per dimension), there is no noticeable difference compared to the complex-valued continuous Gaussian distribution, which is a very good approximation for OFDM. Consequently, in case of powerful signal shaping, the best possible PAR behavior is achieved in case of ideal low-pass filtering, corresponding to a wide-sense stationary complex-valued transmit signal.

In order to visualize the impact of an increase in transmission rate, we also consider the distributions of IP for $R = 4$ per dimension, i.e., 16ASK and 256QAM as baseline. For real-valued modulation, the corresponding iccdf curves are depicted in Fig. 7, and for the complex-valued case in Fig. 10. It can be seen that in each case the PAR behavior of the shaped constellations approaches that of the continuous Gaussian one even faster as compared to rate $R = 2$ per dimension; larger shaped constellations approximate a continuous Gaussian density much better then small constellations. Besides this, basically the same observations as above can be made.

From the results, the well-known trade-off between average transmit power and peak-to-average power ratio [3] is clearly visible; illustrated in Fig. 11. Uniformly drawn coefficients exhibit a relatively low PAR, but at the cost of a high transmit power (no shaping gain). Via the application of signal shaping the average power is decreased (i.e, a shaping gain is achieved) at the cost of the PAR behavior. E.g., a shaped constellation with $\tilde{M} = 20$ coefficients per dimension yields a shaping gain of about 1.4 dB compared to 16ASK/256QAM, but leads to a growth in PAR of about 2.5 to 3 dB. An even larger increase of the shaping cardinality provides only marginal additional shaping gain but further enlarges the PAR.

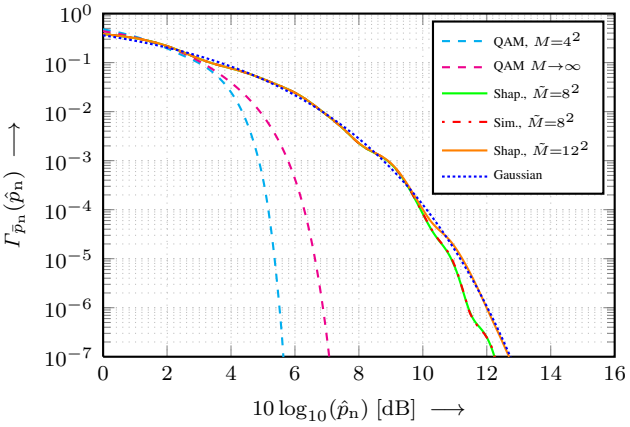

Fig. 8. Time-averaged ccdf of the normalized instantaneous power for complex-valued modulation of rate $R = 4$ (RRC, $\alpha = 0.45$). In case of shaping with $\tilde{M} = 8^2 = 64$, the result obtained by Monte-Carlo simulation is also shown.

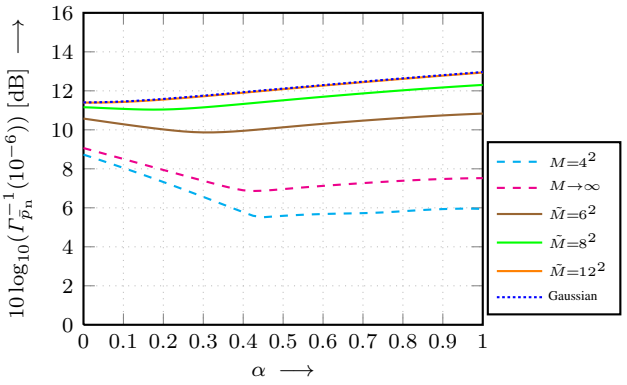

Fig. 9. Time-averaged iccdf of the normalized instantaneous power at probability $\psi = 10^{-6}$ over the roll-off factor α. Complex-valued modulation with rate $R = 4$. Dashed (cyan, magenta): conventional QAM; solid: shaped constellations; dotted blue: two-dimensional continuous Gaussian pdf.

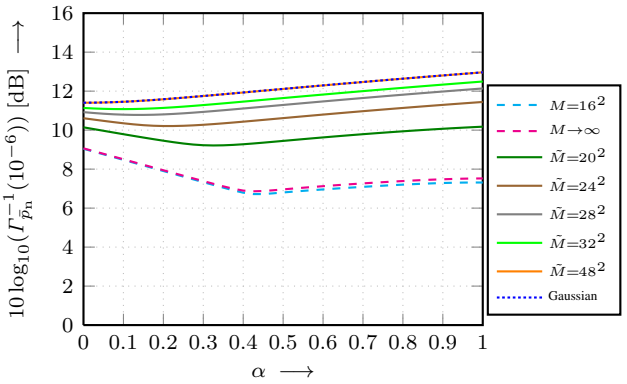

Fig. 10. Time-averaged iccdf of the normalized instantaneous power at probability $\psi = 10^{-6}$ over the roll-off factor α. Complex-valued modulation with rate $R = 8$. Dashed (cyan, magenta): conventional QAM; solid: shaped constellations; dotted blue: two-dimensional continuous Gaussian pdf.

Continuous Gaussian coefficients, which (approximately) occur in case of OFDM or an extensive signal shaping, achieve the maximum possible shaping gain (*ultimate*

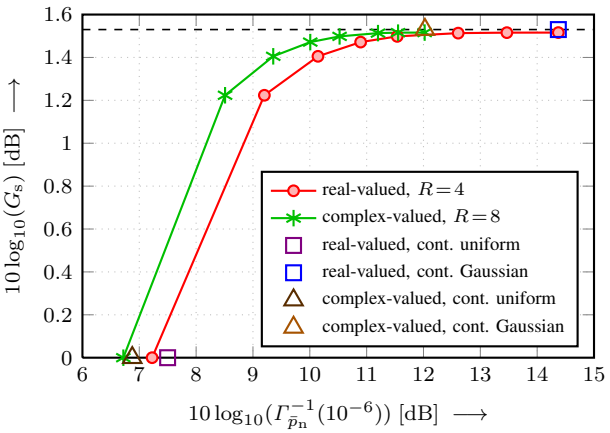

Fig. 11. Relationship between the PAR via iccdf at probability $\psi = 10^{-6}$ and the achievable shaping gain G_s. The values for 16ASK ($R = 4$) and 256QAM ($R = 8$) are shown as references (no shaping gain). Results of related shaped constellations (data rates constant) with cardinalities $\tilde{M} = 18, 20, 22, 24, 28, 32, 48$ per dimension are shown in ascending order (concerning both aspects). Moreover, the continuous uniform distribution is compared to the continuous Gaussian one for both the real- and complex-valued case.

shaping gain) of 1.53 dB [3], but would lead to a very large PAR (for finite probabilities ψ; for $\psi \to 0$ the PAR even tends to infinity).

In summary, signal shaping closes the gap between the PAR behavior of single-carrier modulation and multi-carrier transmission via OFDM. As already mentioned in [13], the (discrete) uniform distribution of coefficients for conventional single-carrier schemes basically results in a superior behavior compared to the (nearly) continuous Gaussian case. The application of signal shaping increases the PAR to the level of OFDM but, in contrast to OFDM, a shaping gain (reduction in average transmit power) is possible. Finally, shaping can also be applied in OFDM (e.g., [2]); here without a further degradation in PAR performance.

V. Conclusion

Approaches for the assessment of the PAR behavior have been presented for conventional single-carrier schemes, for single-carrier modulation employing signal shaping, and for multi-carrier transmissions via OFDM. In particular, strategies for the computation of the statistical distributions of the (normalized) instantaneous power have been worked out. Using these tools, the PAR behavior of all modulation techniques can be compared.

It has been shown that the application of signal shaping results in an inferior PAR behavior compared to conventional (unshaped) single-carrier schemes. Achieving large shaping gains requires a sufficient constellation expansion; in turn the shaped constellations closely approximate a continuous Gaussian distribution, and, hence, coincide with the situation in OFDM. The trade-off between average transmit power and the peak-to-average power has been discussed.

In summary, considering advanced single-carrier and multi-carrier transmission systems, the PAR performance is identical in principle. Via unused tones (guard bands) an almost perfect rectangular spectrum is practically possible in OFDM; for pulse shaping in single-carrier schemes a non-zero roll-off factor has to be used. Since $\alpha = 0$ is the best case for Gaussian amplitude coefficients, OFDM even has a slight advantage over shaped single-carrier schemes.

References

[1] J.A.C. Bingham. Multicarrier Modulation for Data Transmission: An Idea Whose Time Has Come. *IEEE Commun. Mag.*, pp. 5–14, May 1990.

[2] M. Bossert, A. Donder. On the Effects of Trellis Shaping in OFDM Systems. *Annales des Télécommunications*, pp. 74–80, Jan./Feb. 1997.

[3] R.F.H. Fischer. *Precoding and Signal Shaping for Digital Transmission*. John Wiley & Sons, New York, 2002.

[4] W.A. Gardner, L. Franks. Characterization of Cyclostationary Random Signal Processes. *IEEE Trans. Inf. Theory*, pp. 4–14, Jan. 1975.

[5] I. Gutman, D. Wulich. Distribution of Instantaneous Power in Single Carrier Signal with Independent I/Q Components. *IEEE Trans. Wireless Commun.*, pp. 3660–3667, Oct. 2012.

[6] S. Müller, R. Bäuml, R.F.H. Fischer, J.B. Huber. OFDM with Reduced Peak-to-Average Power Ratio by Multiple Signal Representation. *Annales des Télécommunications*, pp. 58–67, Feb. 1997.

[7] H. Ochiai, H. Imai. On the Distribution of the Peak-to-Average Power Ratio in OFDM Signals. *IEEE Trans. Commun.*, pp. 282–289, Feb. 2001.

[8] H. Ochiai. Exact and Approximate Distributions of Instantaneous Power for Pulse-Shaped Single-Carrier Signals. *IEEE Trans. Wireless Commun.*, pp. 682–692, Feb. 2011.

[9] A. Papoulis, S.U. Pillai. *Probability, Random Variables and Stochastic Processes*. Fourth Edition, McGraw-Hill, New York, 2002.

[10] J.G. Proakis, M. Salehi. *Digital Communications*. Fifth Edition, McGraw-Hill, New York, 2007.

[11] S. Shepherd, J. Orriss, S. Barton. Asymptotic Limits in Peak Envelope Power Reduction by Redundant Coding in Orthogonal Frequency-Division Multiplex Modulation. *IEEE Trans. Commun.*, pp. 5–10, Jan. 1998.

[12] C. Siegl. *Peak-to-average Power Ratio Reduction in Multi-antenna OFDM Via Multiple Signal Representation*. PhD Thesis, University of Erlangen-Nuremberg, 2010.

[13] S. Stern, R.F.H. Fischer. Efficient Assessment of the Instantaneous Power Distributions of Pulse-Shaped Single- and Multi-Carrier Signals. *Proceedings of First International Black Sea Conference on Communications and Networking*, pp. 12–17, July 2013.

[14] M. Tanahashi, H. Ochiai. On the Distribution of Instantenous Power in Single-Carrier Signals. *IEEE Trans. Wireless Commun.*, pp. 1207–1215, Mar. 2010.

[15] D. Wulich, L. Goldfeld. Bound of the Distribution of Instantaneous Power in Single Carrier Modulation. *IEEE Trans. Wireless Commun.*, pp. 1773–1778, July 2005.

[16] G. Wunder, H. Boche. Upper Bounds on the Statistical Distribution of the Crest-Factor in OFDM Transmission. *IEEE Trans. Inf. Theory*, pp. 488–494, Feb. 2003.